From Earthquake Centroid to Spatial-Temporal Rupture Evolution: Mw 6.3 Movri Mountain Earthquake, June 8, 2008, Greece

F. Gallovič,[1,2] J. Zahradník,[1] D. Křížová,[1] V. Plicka,[1] E. Sokos,[3] A. Serpetsidaki,[3] and G-A. Tselentis,[3]

We propose a new strategy to reveal the spatial-temporal evolution of the earthquake rupture process from near-regional data, without assuming a constant rupture velocity. The approach is based on a conjugate gradient method, for which we express analytically the required waveform-misfit derivative with respect to slip on the fault. The derivative is given by back-propagation of residual seismograms towards the source. A good initial source approximation is necessary, being obtained from hypocenter location and centroid-moment tensor solution. The iterative approach then gradually reveals major characteristics of the source process. As an application, we investigate a line source model of a damaging Mw6.3 earthquake in Greece, revealing predominantly unilateral rupture propagation and two or three main slip patches, one of which being significantly delayed, indicating a temporary rupture arrest. The region of largest slip coincides with the region of least abundant aftershocks between hypocenter and centroid. The method has application potential for shakemaps, emergency response, and/or aftershock hazard assessment.

1. Introduction

Retrieval of earthquake source parameters is primarily needed for better insight into the physics of the faulting process. However, these parameters are useful also in practical real-time application, such as generating accurate shakemaps and planning emergency response [*Wald et al.*, 1999; *Convertito et al.*, 2008]. Many observational studies and numerical simulations [*Gallovič and Brokešová*, 2004; *Wang et al.*, 2008] further confirmed the importance of such parameters as the direction of the rupture propagation and position of main asperities since they dramatically affect the strong ground motions, see also *Mai* [2009] and references therein. Another application requiring accurate source parameters in near real-time is the aftershock hazard assessment [*Gerstenberger et al.*, 2005; *Gallovič and Brokešová*, 2008].

Regional earthquake studies usually comprise hypocenter determination and calculation of the centroid-moment tensor (CMT), which represents a first-order approximation of the source process. Discriminating the fault plane out of the two nodal planes might follow, possibly complemented with a discrete representation of the earthquake by multiple point-sources. Further step is a gross estimation of the spatial-temporal rupture evolution in terms of, e.g., second-order moment tensors [*McGuire et al.*, 2002], slip patches [*Vallee and Bouchon*, 2004] or continuous representation of the rupture evolution. For example, *Dreger and Kaverina* [2000] seek the best-fitting constant rupture velocity and rise time to reveal the continuous slip distribution on the fault. However, such parameterizations might bias the inverted slip model when the rupture evolution violates the simplifying presumptions.

The present paper introduces a new non-parametric method to extend source models from their first-order approximation (CMT) to a more insightful image of the rupture evolution. *Larmat et al.* [2006] and *Ishii et al.* [2005] used seismic source time-reversal imaging, showing that back-propagated records refocus seismic waves at the right location and time of the earthquake. By a similar approach *Allmann and Shearer* [2007] localized a high-frequency asperity of the 2004 Parkfield earthquake. In our approach, starting from an initial source model based on the CMT solution, we back-propagate residual seismograms to obtain subsequent models by iteration, using a conjugate gradients technique. The new inversion strategy is applied to a damaging earthquake in Greece.

2. Method of iterative slip inversion

Based on recent adjoint tomographic methods [*Tromp et al.*, 2005], we address the earthquake rupture evolution from a similar viewpoint: the gradient of the waveform misfit with respect to the model parameters is analytically derived, which enables efficient minimization by routine methods of conjugate gradients. For simplicity, we assume a line fault of length L and formal width W, $L >> W$. The j-th component of the synthetic seismogram $u_j(\boldsymbol{x}_i, t)$ at receiver $\boldsymbol{x}_i$ can be expressed by the representation theorem [*Aki and Richards*, 2002], i.e. by integration over the fault coordinate ξ of the slip velocity $s(\xi, t)$, varying with time t, convolved with the impulse response of the medium $H(\boldsymbol{x}_i; \xi, t)$ for a predetermined double-couple mechanism.

We seek to estimate slip velocity $s(\xi, t)$ without any parameterizations of its spatial-temporal distribution (except its numerical discretization by piece-wise constant basis functions). Misfit is defined as an L2 norm between synthetic and observed seismograms, with an additional stabilizing constraint on the scalar seismic moment, assumed to have a predetermined value M_{0fix} (from a previous CMT analysis),

$$\Lambda = \frac{1}{2L_u} \int_0^T \sum_{i,j} \left[u_j(\boldsymbol{x}_i, t) - u_j^{obs}(\boldsymbol{x}_i, t) \right]^2 dt - \frac{1}{2M_{0fix}^2} \left[M_0 - M_{0fix} \right]^2 . \quad (1)$$

[1]Charles University in Prague, Faculty of Mathematics and Physics, Department of Geophysics, Czech Republic
[2]Universita degli Studi "Federico II" di Napoli, Department of Physics, Italy
[3]University of Patras, Geology Department, Seismological Laboratory, Greece

0094-8276/09/$5.00

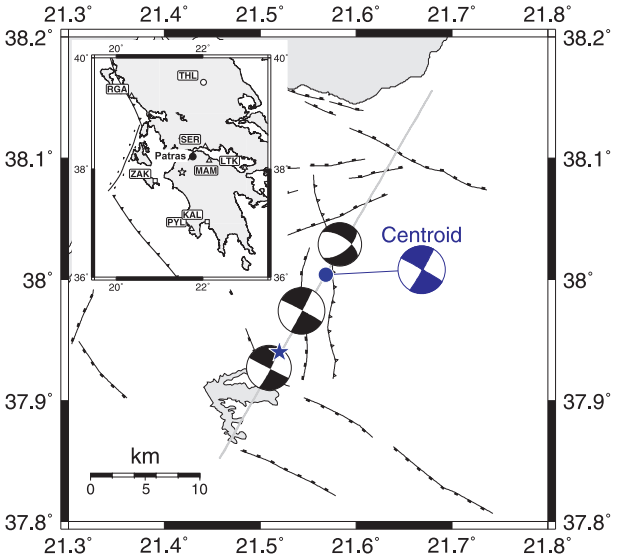

Figure 1. Two discrete representations of the 2008 Movri Mountain earthquake. A single point-source model (blue circle and beach ball scaled with respect to magnitude) and extended model composed of three point-sources. The blue star represents the epicenter. The grey line is the assumed fault, strike 30^o, depth 17 km. The inset shows the stations used. Data from unclipped broadband velocigraphs (THL, RGA) and strong motion accelerographs (remaining stations) were used. Note that none of the local faults simply relates with this earthquake [*Koukouvelas et al.*, 2009].

The normalizing factor L_u is the L2 data norm. The Fréchet differential of the misfit Λ can be expressed as

$$D\Lambda = \int_0^T \int_0^L \left(\frac{1}{L_u} \sum_{i,j} H(\boldsymbol{x}_i; \xi, -t) \star \left[u_j(\boldsymbol{x}_i, t) - u_j^{obs}(\boldsymbol{x}_i, t) \right] - \frac{1}{M_{0fix}^2} \left[M_0 - M_{0fix} \right] \mu W \right) Ds(\xi, t) d\xi dt \quad (2)$$

with rigidity denoted as μ. Equation (2) relates a small change of misfit $D\Lambda$ to small changes in the slip model $Ds(\xi, t)$ via the kernel in round brackets in which residual seismograms $u_j - u_j^{obs}$ are back-propagated in time towards the source. Furthermore, assuming the slip velocity function to be non-negative, we substitute $Ds(\xi, t) = s(\xi, t) D(\ln s(\xi, t))$; this is an implicit positivity constraint [*Tarantola*, 1987]. Equation (2) is the key ingredient for the minimization of Λ by the conjugate gradient method [*Press et al.*, 1992]. The inversion procedure is non-linear and iterative; it should start from a good first approximation, in our case represented by the CMT solution. For the complete derivation of equation (2) and the final discretized formula, see the electronic supplement. Note also that generalization to 2D fault models is straightforward. The line-fault approximation was chosen due to a poor depth resolution in the present application.

3. Application to the 2008 Movri Mountain earthquake

On June 8, 2008 (12:25 UTC) an Mw6.3 strike-slip earthquake occurred in the north-western Peloponnese (Greece) without clear relation to mapped faults, but as close as ~30 km from Patras, the third major city of Greece [*Ganas et al.*, 2009]. Two victims were reported, along with hundreds of injuries and extensive damage, mainly in non-

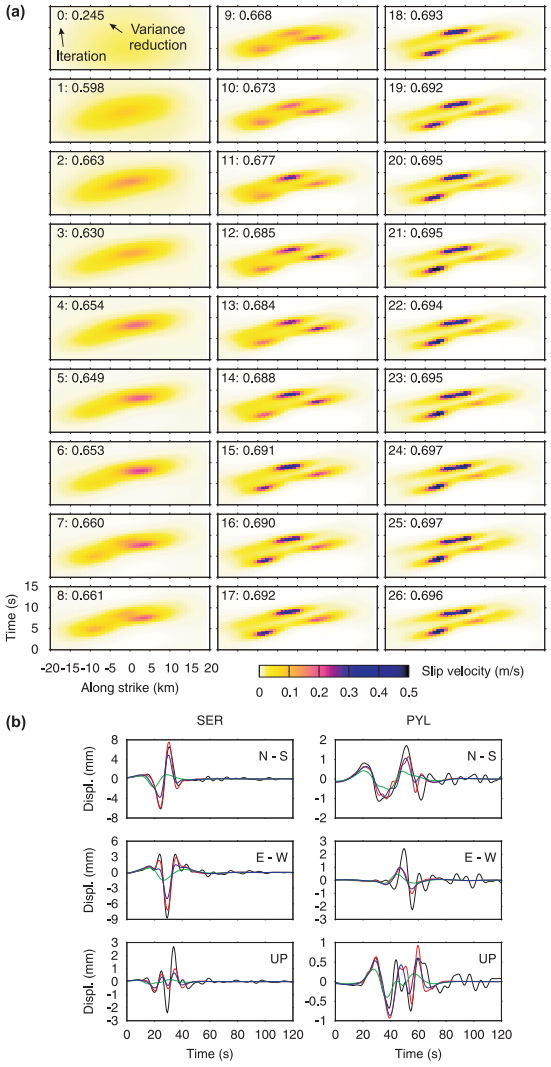

Figure 2. Continuous representation of the 2008 Movri Mountain earthquake based on the iterative method introduced in this paper. (a) Each frame visualizes one iteration of the temporal variation of the slip velocity along the line fault. Frame 0 is the starting model developed from the CMT model of Figure 1. In general, the iterations first show a single patch and reveal direction of the rupture propagation (from left to right), then decompose the slip into main asperities, and finally tend to focus each of them. (b) Matching data with synthetics. Near regional waveforms up to 0.2 Hz, corrected for instrument response, plotted in black for stations SER and PYL, are compared with synthetic seismograms for three selected iterations: 0 (green), 1 (blue) and 26 (red). Same comparison for other stations is presented in the electronic supplement (Figure A3).

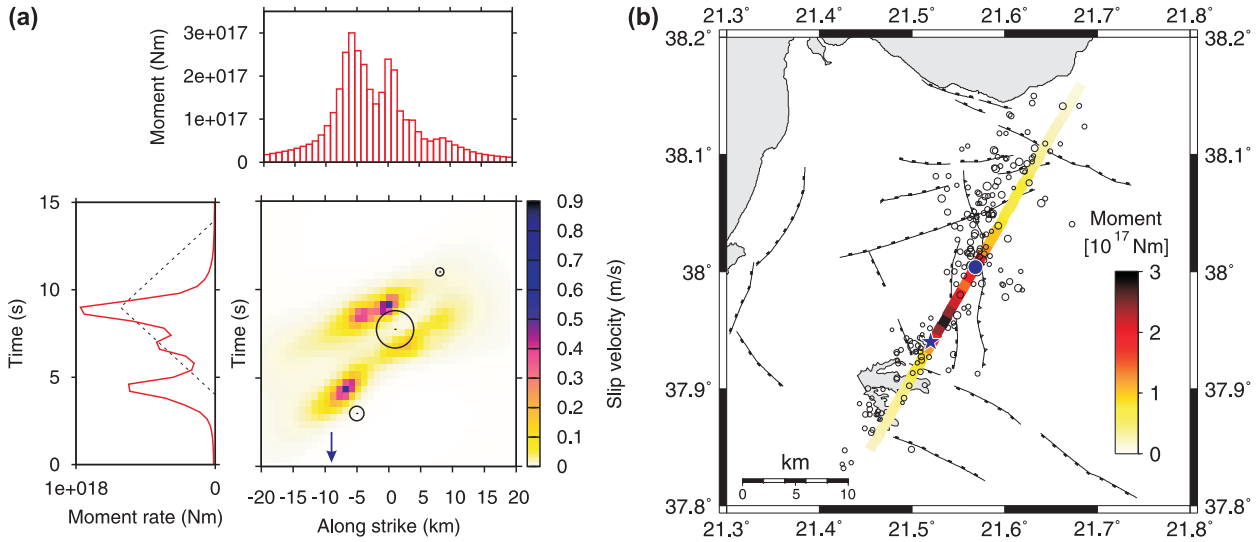

Figure 3. (a) Comparison of the continuous and discrete models. The distribution of the slip velocity along strike of the line fault (x-axis) and time (y-axis) for the 26$^{\text{th}}$ iteration (see Figure 2), in color, is superimposed with the three point-source subevents (black circles scaled with respect to scalar moment) from Figure 1. Blue arrow on the along-strike axis denotes epicenter (−8 km), while centroid is at 0 km. The left and top panels (red lines) show the integrals of the color figure with respect to space and time, respectively. The dashed line in the left panel represents the single point-source (centroid) solution. (b) Comparison between the continuous source model and the aftershocks relocated by double-difference method [*Waldhauser and Ellsworth*, 2000]. The moment distribution inverted in this study (from the top panel of Figure 3a) is plotted onto the map projection of the steeply dipping fault plane. The aftershocks (small black circles) are least abundant in the maximum slip region located between the centroid (blue circle) and epicenter (blue star).

reinforced buildings. Although strong earthquakes are common in western Greece, this event took place in a region free of strong events throughout the historic observation period. The earthquake was followed by aftershock sequence with an irregular distribution, composed of at least two clusters.

To investigate the Movri Mountain earthquake we proceeded in a *cascade* of the following procedures. First, the hypocenter was relocated at 37.94^{o}N, 21.52^{o}E, depth 19 km, 12:25:28.15 UTC. Then waveforms from eight near-regional stations (see Figure 1), band-pass filtered 0.01-0.2 Hz, were inverted for the deviatoric CMT using the ISOLA code [*Sokos and Zahradník*, 2008]: centroid position 38.00^{o}N, 21.57^{o}E, depth 17 km, 12:25:35.5 UTC, strike/dip/rake = 31^o/84^o/-179^o, double-couple percentage 90%, scalar moment $3.4 \cdot 10^{18}$ Nm. The theoretical impulse responses were calculated in a layered crustal model [*Haslinger et al.*, 1999] using the discrete wavenumber method [*Bouchon*, 1981]. Second, following the H-C method [*Zahradník et al.*, 2008], the hypocenter and centroid were combined to identify the north-east south-west trending fault plane, without waiting for aftershocks; the rupture propagation direction was also indicated by the relative position of the hypocenter and centroid (Figure 1). Then, a multiple point-source solution, similar to *Zahradník et al.* [2005], was calculated again with the ISOLA code along a 40 km trial line passing through the centroid position. It revealed three significant contributions of a rather stable focal mechanism (Figure 1); the cumulative scalar moment was equivalent to the CMT solution.

At this point, the new method described above is utilized. The centroid position, and time, along with its focal mechanism and scalar seismic moment from the previous steps are used as a first order approximation of the line source model (see Figure 2a, top left frame). We use the same frequency band and set of stations as for the initial three-point-source modeling. Progress of the slip-inversion iterations is shown in Figure 2a. During the first iteration steps the overall rupture-propagation direction emerges, while at later steps the slip becomes portioned, and the fit slightly increases. Starting from the 18$^{\text{th}}$ iteration, the slip model does not change much. Figure A1 in the electronic supplement shows a synthetic test resembling the inverted model. The iterative process is remarkably similar, also suggesting the asperity splitting in the later iteration steps.

The waveform match of the final model has an overall variance reduction of 0.7. Figure 2b demonstrates details of the waveform fitting at two stations (PYL and SER); fit for other stations is presented in the electronic supplement (Figure A3). Figure A4 in the electronic supplement shows the waveform match for the 26$^{\text{th}}$ iteration of the new method and the CMT solution with main improvement in the duration of the dominant pulses of the records. Note that not all stations are equally sensitive to the rupture evolution. For example, the rupture propagation direction revealed in the first iterations are constrained by the stations lying along the fault line (SER, MAM, ZAK). Later, after this major contribution is removed from the data, coherent information from all stations suggests the splitting of the asperities.

Figure 3a shows again the more or less arbitrarily chosen 26$^{\text{th}}$ iteration as the final model. Note that similar result was obtained when using a different crustal model and repeatedly removing each station (jack-knifing). The slip evolution exhibits predominantly unilateral rupture propagation (to the north-east) along a 20 km long segment of the fault, at a velocity of about 3 km/s starting close to the (independently determined) hypocenter. It is to emphasize that these features are data driven, and not constrained a priori. The slip velocity has at least two or three main episodes that roughly correlate with the previous three-point source model. Nevertheless, compared to the point sources, the patches found by the new method provide a considerably deeper insight into the spatial-temporal rupture evolution. An interesting finding is that one of the slip episodes features a significant time delay, most likely caused by a temporary rupture arrest. Note that such results could not be easily obtained with methods constraining the rupture velocity at a constant value.

4. Discussion and Conclusions

In this study, a new iterative slip-inversion method based on back-propagation of residual seismograms is proposed. As an application, we investigate a recent damaging 2008 Mw6.3 earthquake in Greece, using near-regional data. The inversion method requires an initial approximation of the seismic source, which we obtain in cascade of operations: hypocenter relocation and determination of the centroid position and focal mechanism, complemented by identification of the fault plane. The iterative approach then gradually reveals major characteristics of the source process such as direction of the rupture propagation and dominant asperities.

Figure 3b shows the final slip model from Figure 3a on a map in relation to the double-difference relocated aftershocks. The largest slip coincides with the region of the least abundant aftershocks (almost a gap), between hypocenter and centroid. Note that the north-east and south-west clusters of aftershocks differ in several aspects: The former group comprised events up to M 4.4, the latter contained only smaller magnitudes (M<3.3). Moreover, first event of M≥3 occurred in the south-western group as late as 13 hours after the mainshock, while, during the same period, there were more than 30 such events in the north-eastern group. We speculate that the north-eastern aftershocks might have been boosted by the predominantly unilateral rupture propagation, but a detailed study would require dynamic rupture modeling.

The cascade methodology and the iterative slip inversion were primarily developed for obtaining gross features of the extended seismic source, extractable from near-regional waveforms at relatively low frequencies. Such data have recently been broadly available in near-real time. Finer details of the rupture evolution would require higher frequencies, local strong-motion stations, and significantly better constrained crustal models; as a rule, except a few densely instrumented regions of the world, such data are available only a considerable time after the event, thus preventing a near real-time analysis of the rupture process.

The new methodology has two main advantages: (i) It provides a stable estimate of the rupture evolution (without splitting the slip pattern into ill-conditioned details). Robustness comes from the positivity constraint, fixed moment and a good initial approximation. (ii) It is quite fast, taking minutes on a PC. As such it has a strong application potential in shakemaps, emergency response, and/or in aftershock hazard assessment.

Acknowledgments. Martin Mai and an anonymous reviewer helped to improve the manuscript. The authors acknowledge free Internet access of waveforms provided by NOA (THL) and ITSAK (stations ZAK, KAL); special thanks to Ch. Papaioannou. The remaining stations (RGA, MAM, SER, LTK, PYL) belong to the PSLNET network. Financial support: GAČR 205/07/0502, GAČR 205/08/P013, MSM0021620860, GAUK 14509. This research has benefited from funding provided by the Italian Presidenza del Consiglio dei Ministri - Dipartimento della Protezione Civile (DPC). Scientific papers funded by DPC do not represent its official opinion and policies.

References

Aki, K., and P. G. Richards (2002), *Quantitative Seismology*, University Science Books, Sausalito, California.

Allmann, B.P., and P. M. Shearer (2007), A High-Frequency Secondary Event During the 2004 Parkfield Earthquake, *Science*, *318*, 1279–1283.

Bouchon, M. (1981), A simple method to calculate Green's functions for elastic layered media, *Bull. Seism. Soc. Am.*, *71*, 959–971.

Convertito, V., R. De Matteis, L. Cantore, A. Zollo, G. Iannaccone, and M. Caccavale (2009), Rapid estimation of ground-shaking maps for seismic emergency management in the Campania Region of southern Italy, *Nat. Hazards*, in press.

Dreger, D., and A. Kaverina (2000), Seismic Remote Sensing for the Earthquake Source Process and Near-Source Strong Shaking: A Case Study of the October 16, 1999 Hector Mine Earthquake, *Geophys. Res. Lett.*, *27*, 1941–1944.

Gallovič, F., and J. Brokešová (2004), The k^{-2} rupture model parametric study: example of the 1999 Athens earthquake, *Studia geoph. et geod.*, *48*, 589–613.

Gallovič, F., and J. Brokešová (2008), Probabilistic aftershock hazard assessment II: Application of strong ground motion modeling, *J. Seismology*, *12*, 65–78.

Ganas, A., E. Serpelloni, G. Drakatos, M. Kolligri, I. Adamis, Ch. Tsimi, and E. Batsi (2009), The Mw 6.4 SW-Achaia (western Greece) earthquake of 8 June 2008: Seismological, field, GPS observations and stress modeling, *J. Earthq. Eng.*, in press.

Gerstenberger, M.C., S. Wiemer, L. M. Jones, and P. A. Reasenberg (2005), Real-time forecasts of tomorrow's earthquakes in California, *Nature*, *435*, 328-331.

Haslinger, F., E. Kissling, J. Ansorge, D. Hatzfeld, E. Papadimitriou, V. Karakostas, K. Makropoulos, H.-G. Kahle, and Y. Peter (1999), 3D crustal structure from local earthquake tomography around the Gulf of Arta (Ionian region, NW Greece), *Tectonophysics*, *304*, 201–218.

Ishii, M., P. M. Shearer, H. Houston, and J. E. Vidale (2005), Extent, duration and speed of the 2004 Sumatra Andaman earthquake imaged by the Hi-Net array, *Nature*, *435*, 933-936.

Klein, F. W. (2002), User's guide to HYPOINVERSE-2000, a FORTRAN program to solve earthquake locations and magnitudes, *U. S. Geological Survey Open File Report*, *02-171*, Version 1.0.

Koukouvelas, I. K., S. Kokkalas, and P. Xypolias (2009), Surface deformation during the Mw 6.4 (8 June 2008) Movri Mountain earthquake in the Peloponnese, and its implications for the seismotectonics of western Greece, *Int. Geol. Rev.*, , in press.

Larmat, C., J.-P. Montagner, M. Fink, Y. Capdeville, A. Tourin, and E. Clé vé dé (2006), Time-reversal imaging of seismic sources and application to the great Sumatra earthquake, *Geophys. Res. Lett.*, *33*, L19312.

Mai, M. (2009), Ground Motion: Complexity and Scaling in the Near Field of Earthquake Ruptures, *Encyclopedia of Complexity and Systems Science, W.H.K. Lee and R. Meyers (Eds.)*, Springer, 4435–4474.

McGuire, J. J., L. Zhao, and T. H. Jordan (2002), Predominance of Unilateral Rupture for a Global Catalog of Large Earthquakes, *Bull. Seism. Soc. Am.*, *92*, 3309–3317.

Press, W. H., B. P. Flannery, S. A. Teukolsky, and W. T. Vetterling (1992), *Numerical Recipes in Fortran, The Art of Scientific Computing, 2nd ed.*, Cambridge University Press, New York.

Sokos, E., and J. Zahradník (2008), ISOLA A Fortran code and a Matlab GUI to perform multiple-point source inversion of seismic data, *Computers & Geosciences*, *34*, 967-977.

Tarantola, A. (1987), *Inverse Problem Theory: Methods for Data Fitting and Model Parameter Estimation*, Elsevier Science Publishers, Science Publishers, Amsterdam.

Tromp, J., C. Tape, and Q. Liu (2005), Seismic tomography, adjoint methods, time reversal and banana-doughnut kernels, *Geophys. J. Int.*, *160*, 195–216.

Valle, M., and M. Bouchon (2004), Imaging coseismic rupture in far field by slip patches, *Geophys. J. Int.*, *156*, 615-630.

Wald, D. J., V. Quitoriano, T. H. Heaton, H. Kanamori, C. W. Scrivner, C. B. Worden (1999), TriNet shakemaps: rapid generation of instrumental ground motion and intensity maps for earthquakes in southern California, *Earthq. Spectra*, *15*, 537–555.

Waldhauser, F., and W. L. Ellsworth (2000), A Double-Difference Earthquake Location Algorithm: Method and Application to the Northern Hayward Fault, *Bull. Seism. Soc. Am.*, *90*, 1353–1368.

Wang, H., H. Igel, F. Gallovič, A. Cochard, and M. Ewald (2008), Source-Related Variations of Ground Motions in 3-D media: Application to the Newport-Inglewood Fault, Los Angeles Basin, *Geophys. J. Int.*, *175*, 202–214.

Zahradník, J., A. Serpetsidaki, E. Sokos, and G-A. Tselentis (2005), Iterative deconvolution of regional waveforms and a double-event interpretation of the 2003 Lefkada earthquake, Greece, *Bull. Seism. Soc. Am.*, *95*, 159–172.

Zahradník, J., F. Gallovič, E. Sokos, A. Serpetsidaki, and G-A. Tselentis (2008), Quick fault-plane identification by a geometrical method: application to the Mw6.2 Leonidio earthquake, January 6, 2008, Greece, *Seism. Res. Lett.*, *79*, 653–662.

F. Gallovič, Department of Geophysics, Faculty of Mathematics and Physics, Charles University, V Holešovičkách 2, Praha 8, 180 00, Czech Republic. (gallovic@karel.troja.mff.cuni.cz)